Dark-exciton giant Rabi oscillations with no external magnetic field

Vladimir Vargas-Calderón * and Herbert Vinck-Posada
Grupo de Superconductividad y Nanotecnología, Departamento de Física Universidad Nacional de Colombia, 111321 Bogotá, Colombia

J. M. Villas-Boas
Instituto de Física, Universidade Federal de Uberlândia, 38400-902 Minas Gerais, Brazil

(Received 8 December 2021; revised 28 June 2022; accepted 1 July 2022; published 14 July 2022)

Multiphonon physics is an emerging field that serves as a test bed for fundamental quantum physics and several applications in metrology and on-chip communication, among others. Quantum acoustic cavities or resonators are devices that are being used to study multiphonon phenomena both theoretically and experimentally. In particular, we study a system consisting of a semiconductor quantum dot pumped by a driving laser and coupled to an acoustic cavity. This kind of system has proven to yield interesting multiphonon phenomena, but the description of the quantum dot has been limited to a two-level system. This limitation restrains the complexity that a true semiconductor quantum dot can offer. Instead, in this work we consider a model where the quantum dot can have both bright and dark excitons, the latter being particularly useful due to their lower decoherence rates, because they do not present spontaneous photon emission. In this setup, we demonstrate that by fine-tuning the driving laser frequency, one is able to realize giant Rabi oscillations between the vacuum state and a dark-exciton state with N-phonon bundles. From this, we highlight two outstanding features: first, we are able to create dark-state excitations in the quantum dot without the usual external magnetic field needed to do so; and second, in a dissipative scenario where the acoustic cavity and the quantum dot suffer from losses, the system acts as a phonon gun able to emit N-phonon bundles.

DOI: 10.1103/PhysRevB.106.035305

I. INTRODUCTION

Quantum vibrational modes of solids, described by phonons, have a great potential to be used in technological applications in metrology or quantum information processing [1–6]. Moreover, as the control of individual phonons continues to improve, the study of phonons and their interaction with other excitations in many-body quantum systems is also relevant for testing fundamental physics [7–10]. Analogous to photons in quantum electrodynamics, phonons can be used to store, process, and transduce quantum information. The inclusion of phonons to the quantum toolbox gives a threefold advantage: first, losses by radiation into the electromagnetic field vacuum are no longer present, as phonons can only propagate through some material medium (usually in solid-state devices); second, phonon energy scales are, in general, different from the optical energy scale, making phonons especially suited for on-chip communication [2,4,11,12] in a variety of characteristic energies, from MHz to THz [13–38]; third, many experimental techniques developed by solid-state physicists [7,18,39,40] become available for quantum information processing tasks with phonons [2,12].

Even though the majority of theoretical and experimental efforts have been devoted to single-phonon generation and control, many-phonon states are also required for highly nonclassical sources, useful for quantum sensing and metrology [3] and quantum technologies such as quantum memories and transducers [4–6]. To this end, the recent work by Bin *et al.* [11] proposes a physical system in quantum acoustodynamics composed of a semiconductor quantum dot (QD), modeled as a two-level system, coupled to the phonon mode of an acoustic cavity. The QD is coherently pumped by an external laser with a frequency that can be tuned to excite giant Rabi oscillations between a state that is mostly the vacuum state (no QD excitations and zero phonons in the acoustic cavity) and a state that is composed of an exciton QD state, accompanied by N phonons in the acoustic cavity. The authors then show that dissipative channels allow the emission of N-phonon bundles, and they analyze the quantum statistics of this emission, finding out that, depending on dissipative and Hamiltonian parameters, they can realize a phonon laser or a phonon gun.

In this work we study a QD coherently pumped by an external laser and immersed in an acoustic single-mode cavity [10], but we take into account the richer exciton basis provided by the different spin alignments of the electron and the hole that compose the exciton. Thus, the QD is described by a ground state, two bright-exciton states, and two dark-exciton states. The inclusion of this richer exciton basis allows the description of more complex interactions in the system, which enables the control of interesting phenomena. Therefore, the main contributions of our work, coming from the more complete exciton basis, are the following: dark excitons can be excited, taking advantage of the Bir-Pikus interaction [41], by fine-tuning the laser frequency without the usual need for an external magnetic field [42,43], which is both experimentally challenging and expensive [42,44]; and giant-Rabi

* vvargasc@unal.edu.co

oscillations between a vacuum state and a dark-exciton N-phonon state can be realized to emit N-phonon bundles.

We highlight that the laser-frequency fine-tuning can be performed to target any desired giant Rabi oscillation for a wide range of parameters such as decay rates, characteristic energies and coupling constants. Therefore, the method that we present can be seen as a recipe to produce giant Rabi oscillations. The damping of those oscillations, though, will be determined by the dissipative nature of the physical realization of the embedded QD in an acoustic cavity.

The paper is organized as follows. In Sec. II we introduce the Hamiltonian that models the physical system under consideration. The analysis and discussion of N-phonon bundle emission is presented in Sec. III. We draw conclusions in Sec. IV. Throughout the paper, we use parameters similar in magnitude to those presented in Ref. [11], as this allows us to build a bridge between our results and theirs, allowing a direct comparison of the phenomenology that we find. Nonetheless, some of these parameters are orders of magnitude away from the state-of-the-art experiments involving the coupling of QDs to acoustic cavities. This does not invalidate the rich physics that is described. In fact, as we pointed out, the recipe to produce giant Rabi oscillations is found to hold for more experimentally feasible parameters, as we exemplify and discuss in the Appendix.

II. MODEL

In this work we consider a pumped quantum dot embedded in an acoustic cavity described by the following Hamiltonian [11]:

$$H = H_{\text{QD}} + H_{\text{laser}} + H_{\text{cav}} + H_{\text{el-ph}}. \tag{1}$$

The bare quantum dot is described by a valence state, $|v\rangle$; two bright-exciton states, $|1\rangle$ and $|2\rangle$, with antiparallel electron-hole spins; and two dark-exciton states, $|3\rangle$ and $|4\rangle$, with parallel electron-hole spins. The corresponding Hamiltonian, taking into account the exchange interaction [45,46], and making use of the ladder operators $\sigma_{ij} = |i\rangle\langle j|$, reads [42]

$$\begin{aligned} H_{\text{QD}} = {} & \omega_X(\sigma_{11} + \sigma_{22}) + \omega_d(\sigma_{33} + \sigma_{44}) \\ & + \frac{\delta_1}{2}(\sigma_{12} + \sigma_{21}) + \frac{\delta_2}{2}(\sigma_{34} + \sigma_{43}), \end{aligned} \tag{2}$$

where ω_X is the bare bright-exciton energy, $\omega_d = \omega_X - \delta_0$ is the shifted bare dark-exciton energy, and δ_1 and δ_2 split the bright- and dark-exciton energies. Further, the QD is driven by an external laser that pumps the bright-exciton states through $H_{\text{laser}} = \Omega_1(e^{-i\omega_L t}\sigma_{1v} + e^{i\omega_L t}\sigma_{v1}) + \Omega_2(e^{-i\omega_L t}\sigma_{2v} + e^{i\omega_L t}\sigma_{v2})$. Here, the relative magnitudes of the laser amplitudes Ω_1 and Ω_2 depend on the laser polarization [47]. The time dependence of the whole Hamiltonian is removed in the laser-frequency rotating frame via the unitary transformation $U = \exp(i\omega_L t[\sigma_{11} + \sigma_{22} + \sigma_{33} + \sigma_{44}])$. The acoustic cavity Hamiltonian accounts for the single-phonon mode energy $H_{\text{cav}} = \omega_b b^\dagger b$, where b is the phonon annihilation operator. Throughout the paper we use the values $\delta_0 = 0.04\omega_b$, $\delta_1 = 0.036\omega_b$, and $\delta_2 = 0.01\omega_b$, which match the values reported by Bayer *et al.* [46] for $\omega_b = 5$ meV. Finally, we also consider the coupling of the hole spin to the strain tensor of the QD—described by the Bir-Pikus Hamiltonian [41,48]—as well as the electron-hole exchange interaction [49], resulting in an electron-phonon Hamiltonian that is able to generate phonon-mediated transitions between bright and dark excitons and between the two bright excitons [50]:

$$\begin{aligned} H_{\text{el-ph}} = {} & \left\{ \frac{g_{\text{bd}}}{\sqrt{2}}[(1+i)(\sigma_{13} + \sigma_{14}) + (1-i)(\sigma_{23} + \sigma_{24})] \right. \\ & \left. + g_{\text{bb}}[\sigma_{11} + \sigma_{22} + i(\sigma_{12} - \sigma_{21})] \right\}(b^\dagger + b) + \text{H.c.}, \end{aligned} \tag{3}$$

where $g_{\text{bb(bd)}}$ are bright-bright (bright-dark) exciton coupling rates through phonons. An illustration of the interactions that affect the QD state is given in Fig. 1.

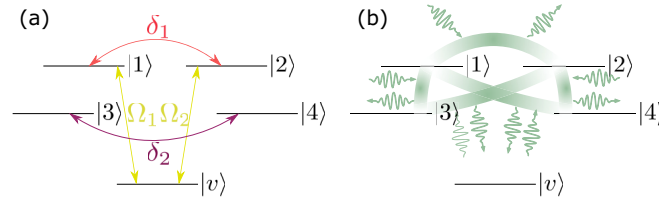

FIG. 1. Interactions that cause transitions between different QD states. Panel (a) shows the interactions portrayed in H_{QD} and H_{laser} with two-directional arrows, and panel (b) shows the interactions portrayed by $H_{\text{el-ph}}$ with gradient-colored lines, which are mediated by phonon absorption and emission processes in the acoustic cavity.

III. RESULTS

Such an electron-phonon coupling, accompanied by the optically driven Stokes process through the laser pumping, allows the excitation of giant Rabi oscillations between the vacuum state $|\text{phonons} = 0\rangle \otimes |\text{QD} = v\rangle$ (for weak laser pumping) and an eigenstate of the Hamiltonian shown in Eq. (1) [11]. In particular, we can select an eigenstate mainly composed of N phonons and dark excitons. As an example, we show in Fig. 2 two such eigenstates that will be used as targets for giant Rabi oscillations.

Giant Rabi oscillations are achieved through a cascading effect [11], where the system transitions from the vacuum state $|0, v\rangle$ to a QD bright-exciton state (depending on the laser amplitudes) and then to a (mostly) dark-exciton symmetric state with N phonons after the system is guided by the electron-phonon coupling mechanism. Examples of such giant Rabi oscillations involving the two- and three-phonon states shown in Fig. 2 can be found in Fig. 3. Both examples show that it is possible to tune the laser frequency to target giant Rabi oscillations between the vacuum state $|0, v\rangle$, and any eigenstate $|\lambda\rangle$ of Eq. (1) by considering a laser frequency $\omega_L = \omega_\lambda - \omega_g$, where $\omega_\lambda = \langle\lambda|H|\lambda\rangle$ and ω_g is its ground-state frequency [51]. It is worth noting that the states

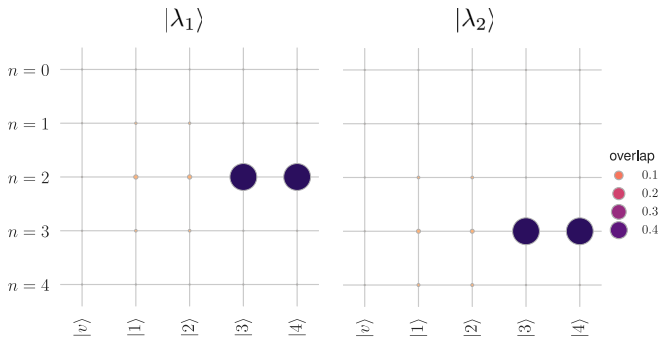

FIG. 2. Eigenstates of Eq. (1) for weak electron-phonon coupling ($g = g_{bb} = g_{bd} \approx 0.02\omega_b$), pumping ($\Omega_1 \approx 0.082\omega_b$, $\Omega_2 = 0$), and the external laser in resonance with the bright-exciton energy ($\omega_L = \omega_X$, where the frequency of the QD can be chosen to match any semiconductor QD exciton energy, e.g., 1.36 eV for GaAs QDs). These values are used throughout the paper, except for the laser frequency, which will be fine-tuned. The state $|*\rangle\lambda_{1(2)}$ is mostly composed by the state $|2(3), d_+\rangle$, where $|d_\pm\rangle = (|3\rangle \pm |4\rangle)/\sqrt{2}$ is the dark-exciton symmetric (+) or antisymmetric (−) state.

$|n, d_-\rangle$, i.e., with antisymmetric dark-exciton matter states, are eigenstates of Eq. (1), but they are not accessible from nondark antisymmetric initial states, as can be easily corroborated by computing $\langle m, \beta|H|n, d_-\rangle = 0$, where $|\beta\rangle$ is any state spanned by bright-exciton states, and m is some number of phonons. However, in the presence of dissipation they can be accessed, as is explored later.

The Hamiltonian analysis so far presented is only relevant to understand the underlying physics of giant Rabi oscillation production, but to study a realistic setup of the proposed system it is necessary to describe it as an open quantum system. Such a description shows that giant Rabi oscillations can emit N-phonon bundles through dissipative channels. In the case of weak coupling to the environment, which leads to the usual Born-Markov approximations

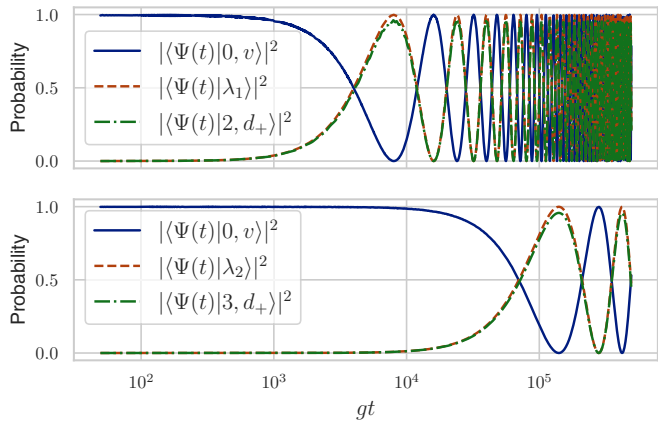

FIG. 3. Giant Rabi oscillations between the zero-phonon valence state (solid line) and the states shown in Fig. 2 (dashed line). The dash-dotted line shows the evolution of the $|n, d_+\rangle$ state for $n = 2$ (top panel) and $n = 3$ (bottom panel). The laser detuning is $\Delta/\omega_b = (\omega_X - \omega_L)/\omega_b \approx -1.960$ for the top panel and ≈ -2.961 for the bottom panel. The same coupling and pumping conditions from Fig. 2 are used.

[52], we consider four dissipative channels under the Gorini-Kossakowski-Sudarshan-Lindblad equation for the system's density operator [53,54]:

$$\frac{d\rho}{dt} = i[\rho, H] + \kappa\mathcal{D}_b[\rho] + \gamma_b \sum_{j=1,2} \mathcal{D}_{\sigma_{vj}}[\rho] + \gamma_d \sum_{j=3,4} \mathcal{D}_{\sigma_{vj}}[\rho] + \gamma_\phi \sum_{j=1}^{4} \mathcal{D}_{\sigma_{jj}}[\rho], \tag{4}$$

where $\mathcal{D}_A[\rho] = A\rho A^\dagger - \frac{1}{2}\rho A^\dagger A - \frac{1}{2}A^\dagger A\rho$ is the dissipator superoperator of the collapse operator A. The four dissipative channels considered in Eq. (4) are as follows: phonon escape from the acoustic nanocavity at a rate κ with a collapse operator b due to unwanted coupling with leaky modes [55,56], spontaneous emission of the bright excitons at a rate γ_b with collapse operators σ_{vj} for $j = 1$ and 2, effective spontaneous emission of the dark excitons (hole or electron spin flip followed by bright-exciton spontaneous emission [57]) at a rate γ_d with collapse operators σ_{vj} for $j = 3$ and 4, and pure dephasing of all exciton states at a rate γ_ϕ with collapse operators σ_{jj} [58].

Solving Eq. (4) using quantum trajectories [59,60] exposes the N-phonon bundle nature of the excitations that are emitted: the N-phonon bundle behaves as a quasiparticle in the context of the dynamical process of emission [61]. Figure 4 depicts this concept by showing a single quantum trajectory that suffers a strongly correlated phonon emission process. The initial state is the vacuum, as shown in Fig. 4(b), right before a quantum jump that takes the system to a dark state with two phonons, as shown in Fig. 4(c). This jump is due to the pure dephasing dissipative channel with a quantum jump operator σ_{44}. The state in Fig. 4(b) is, to a good approximation, $c_+(t)|0, v\rangle + c_-(t)|2, d_+\rangle$, where $|c_+(t)|^2 + |c_-(t)|^2 = 1$. Before the quantum jump, $|c_+(t)|^2 \approx 1$, meaning that the system is still in the vacuum state. The dephasing jump takes the system into a state of two phonons and a dark state, as shown in Fig. 4(c). Now, the phonon dissipative channel—with jump operator b—makes the system undergo a quantum jump through the emission of a phonon, leaving the system in a dark state, but with only one phonon, as shown in Fig. 4(d). The quantum trajectory simulation shows that yet another quantum jump occurs between the points (d) and (e) due to dephasing. This jump, however, does not affect the phonon population. Although the phonon-escape mechanism depletes the cavity phonon-by-phonon, it is shortly after the emission of the first phonon that the second phonon is also emitted due to the jump operator b, leaving the system in a dark-excitonic state with zero phonons, as shown in Fig. 4(e). After the point (e), there are a couple of further dephasing quantum jumps that leave the phonon population unaffected because the exciton already occupies the dark states. Finally, the QD emits a photon due to recombination (jump operator σ_{v3}, which models a random spin flip followed by spontaneous emission), and the system is allowed to transit the same process once again. The two-phonon bundle emission process arises in all quantum trajectories and becomes more common when the electron-phonon coupling g is increased, at the cost of realizing giant Rabi oscillations between the vacuum and states that have a larger bright contribution. Nonetheless, we point

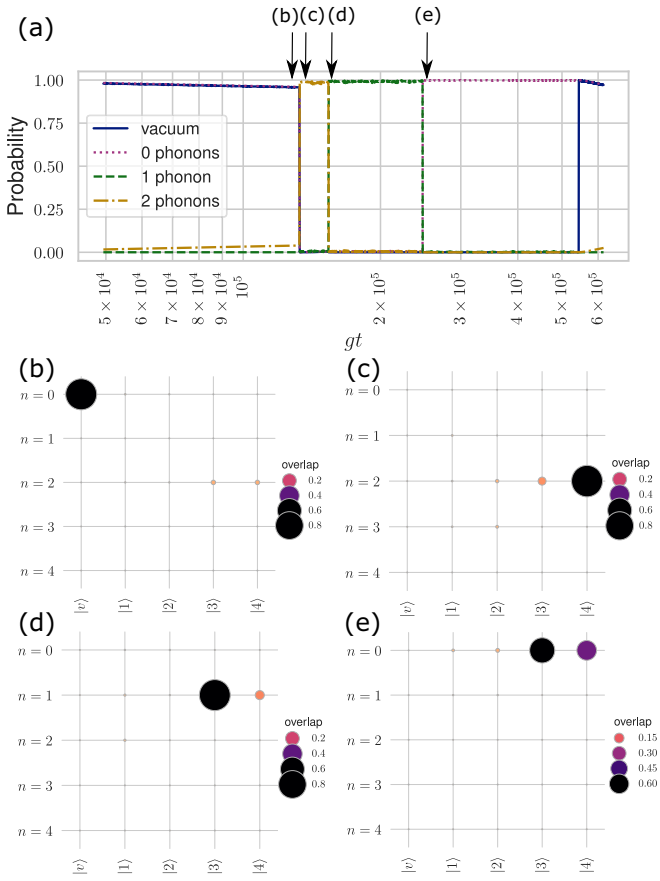

FIG. 4. Evolution of a quantum trajectory due to Hamiltonian dynamics and dissipation-induced quantum jumps. Panel (a) shows the occupation of the vacuum $|0, v\rangle$ state and of the N-phonon states, i.e., the occupation of $\sum_i |N, i\rangle$. Panels (b)–(e) show the state composition of the system at the times pointed out by an arrow in panel (a). The laser detuning is the same as in the top panel of Fig. 3. The dissipative parameters are $\kappa \approx 7.89 \times 10^{-4}\omega_b$, $\gamma_b \approx 1.869 \times 10^{-5}\omega_b$, $\gamma_d = 0.1\gamma_b$, and $\gamma_\phi = 4 \times 10^{-4}\omega_b$. These parameters are used throughout the paper.

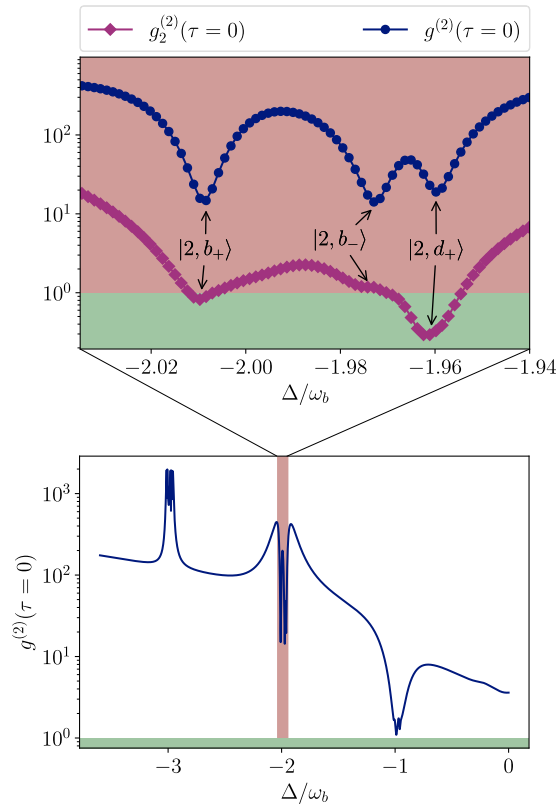

FIG. 5. Equal-time one- and two-phonon bundle correlation functions. At $\Delta \approx -2\omega_b$ there are dips in the superbunching peak of the usual correlation function at resonances corresponding to two-phonon states with bright (anti)symmetric $|b_{(-)+}\rangle$ and with the dark symmetric state $|d_+\rangle$. The red- and green-shaded regions align with sub- and super-Poissonian statistics regions.

out that for the presented parameters, one-phonon emission processes are more common [62].

Moreover, as in the work by Bin *et al.* [11], a signature of strong correlations of the emitted phonons is found in the equal-time nth-order phonon correlation function $g^{(n)}(\tau = 0) = \langle b^{\dagger n} b^n \rangle / \langle b^\dagger b \rangle^n$ [63]. They noticed that near the resonances $\Delta \approx -n\omega_b$ (for $n \geqslant 2$), this correlation function did not show the superbunching peaks that would intuitively be expected for multiphonon emission. Instead, there are dips in the middle of such peaks, as we show in Fig. 5. In their case, only one dip coinciding with the resonance with the $|n, c\rangle$ state was shown because their model was restricted only to one conduction $|c\rangle$ exciton state, whereas in our case, we present three different dips corresponding to the resonances with the bright symmetric and antisymmetric states, as well as the dark symmetric state.

However, such correlation function is not adequate to investigate multiphonon properties associated with the emitted N-phonon bundles. This is due to the fact that the $g^{(2)}(\tau = 0)$ correlation function—normally measured in photonic setups such as the Hanbury Brown and Twiss interferometer [64]—is related to the co-occurrence of single-phonon detection events, as originally derived by Glauber [65]. On the other hand, the equal-time mth-order N-phonon bundle correlation function, defined as $g_N^{(m)}(\tau = 0) = \langle b^{\dagger Nm} b^{Nm} \rangle / \langle b^{\dagger N} b^N \rangle^m$, correctly describes these multiphonon properties because it treats the N-phonon bundle as a quasiparticle [61], with associated creation and annihilation operators $b^{\dagger N}$ and b^N, respectively. In Fig. 5 we show that this generalized correlation function reaches the sub-Poissonian antibunching regime for some values of the laser detuning [66]. The resonance associated with the dark symmetric with the two-phonon state presents the lowest value of $g_2^{(2)}$, well within the antibunching regime. This shows that the Bir-Pikus mechanism allows the generation of robust antibunching behavior when the laser frequency is tuned to target giant Rabi oscillations with the dark symmetric state, even more so than with the usually accessed bright states.

Finally, we examine the phonon emission spectrum [see Fig. 6(c)] to show that the two-phonon emission processes can be frequency resolved. The phonon emission spectrum $I(\omega)$ can be obtained through the Wiener-Khintchine theorem in analogy to the photoluminiscence spectrum: $I(\omega) \propto \frac{\kappa}{\pi} \int_0^\infty \langle b(t) b^\dagger(t + \tau) \rangle e^{i\omega\tau}\, d\tau$ [55,67,68]. We can interpret every single peak through the spectral theory of the Liouvillian

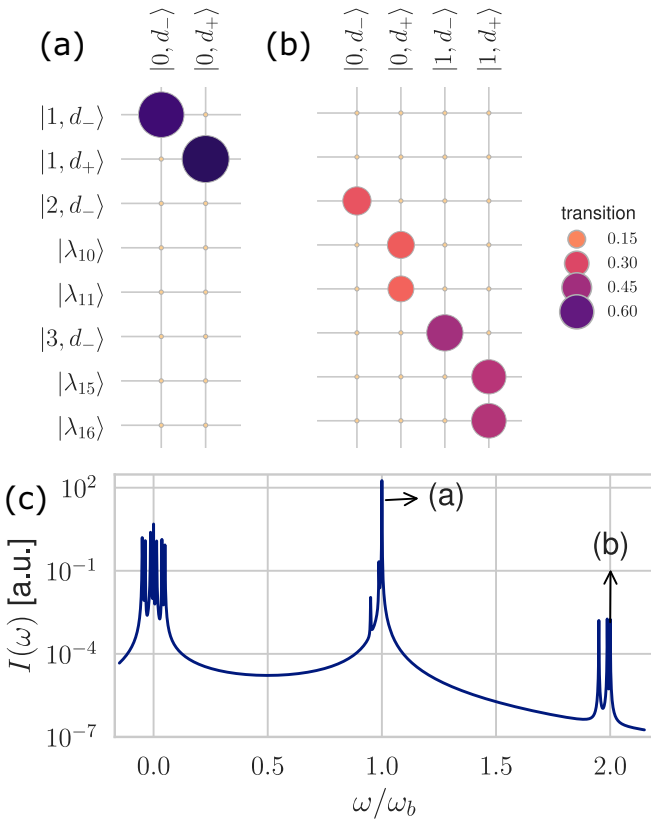

FIG. 6. Phonon emission spectrum $I(\omega)$. Panels (a) and (b) show the elements $|\langle\psi|\varrho|\phi\rangle|^2$ of the Liouvillian eigenmatrices ϱ that match the peaks pointed in the phonon emission spectrum in panel (c). The eigenmatrices show that the peak (a) corresponds to a one-phonon emission process, whereas the peak (b) corresponds to two-phonon emission processes. Eigenstates $|\lambda_{10}\rangle$ and $|\lambda_{11}\rangle$ of Eq. (1) are superpositions of $|0,v\rangle$ and $|2,d_+\rangle$, and eigenstates $|\lambda_{15}\rangle$ and $|\lambda_{16}\rangle$ are superpositions of $|0,v\rangle$ and $|3,d_+\rangle$. The laser detuning is the same as in the top panel of Fig. 3.

superoperator $\mathcal{L}$ that satisfies Eq. (4), written as $\frac{d\rho}{dt} = \mathcal{L}[\rho]$ [69–71]. A formal solution of this equation for a time-independent Liouvillian is $\rho(t) = \sum_k e^{\Lambda_k t}\mathrm{Tr}[\varrho_k\rho(0)]\varrho_k$, where Λ_k are the complex eigenvalues of $\mathcal{L}$ with corresponding eigenmatrices ϱ_k. The eigenvalues are associated with the emission peaks [72–74] as they show both the peak location $\mathrm{Im}\Lambda_k$ and the full-width at half-maximum $-\mathrm{Re}\Lambda_k$. On the other hand, the eigenmatrices account for information about which states are involved in each transition [75]. These transitions can be systematically studied when they involve changes in the number of excitations through dissipative processes only [76–78]. In our case, such a theory cannot be used because of the presence of coherent pumping to the QD. Nonetheless, the examination of the eigenmatrices matrix elements still shows which states are involved in the transitions, as displayed in Figs. 6(a) and 6(b).

Figure 6(a) shows that the most-prominent peak of the spectrum matches transitions between dark states with one phonon and dark states with zero phonons. It is worth noting that the magnitudes of the matrix elements shown in Figs. 6(a) and 6(b) do not indicate the contribution of those transitions to the emission peak. Instead, the excitation of the transitions depends upon the energy injected into the system and the strength of the interactions that enable certain population transfers. Further, Fig. 6(b) shows the allowed transitions for another peak, at a frequency of $\omega = 2\omega_b$, which matches transitions between dark states with two phonons decaying to dark states with no phonons, and also dark states with three phonons decaying to dark states with one phonon. We highlight that the emission peak coinciding with the two-phonon emission is much smaller than the one-phonon emission peak. However, the corresponding transitions can be differentiated due to the large energy difference in the spectrum. For instance, an analogous procedure such as the one presented by Sánchez Muñoz *et al.* [79] can be proposed for phonons. The associated side-bands on each major peak are due to transitions between dark and bright states accompanied by zero-, one-, and two-phonon emission.

IV. CONCLUSIONS

Dark excitons in QDs are more robust to decoherence than bright excitons, because they cannot couple to leaky optical modes. It is usually assumed that dark excitons are produced (and controlled) via external magnetic fields. However, in this work, we show that dark excitons in a QD coherently pumped by a laser and coupled with an acoustic cavity not only can be produced but also can be targeted to realize giant Rabi oscillations between dark states with N phonons and the vacuum. These giant Rabi oscillations show a restricted cascading process that couples states with different phonon numbers, ultimately resulting in an effective coupling between the vacuum and a dark-symmetric-exciton state with N phonons.

In the driven-dissipative scenario, other intermediate states are activated in the cascading process, culminating in N-phonon bundle emission, as shown by analysis of quantum trajectories. Furthermore, we show that N-phonon bundle correlation functions display quantum statistics corresponding to antibunching for the studied parameters, which is a desired property to realize N-phonon guns. Moreover, through the analysis of the emission spectrum, we characterize the acoustic transitions of the system, finding out that N-phonon bundle emission can be frequency resolved, which is an important feature to experimentally distinguish the phonon quasiparticles that escape the acoustic cavity.

Usually, high magnetic fields are needed to control the excitation of dark excitons, and producing these fields requires costly and large apparatuses that endanger the scalability possibilities of these systems. The system theoretically studied in this work provides an important alternative for quantum control in acoustic nanocavities without external magnetic fields to emit multiphonon states through dark-exciton manipulation.

APPENDIX: EXPERIMENTAL FEASIBILITY

So far, we have chosen Hamiltonian and dissipative parameters similar in magnitude to the ones used by Bin *et al.* [11]

because they allow us to make direct comparisons between the phenomenology found in their study and ours. However, these are parameters that are not backed up with the current development of technology and are distant from an actual experimental realization of the proposed N-phonon bundle emission through the excitation of dark-exciton states. As an example, it is true that THz acoustic cavities have been built, but they have not been coupled to QDs. Instead, experiments such as the one by Wigger *et al.* [36] or Nysten *et al.* [80] show that the state-of-the-art has only coupled GHz acoustic cavities to semiconductor QDs. In this section, we show that the phenomenology that we observe still holds for more realistic parameters close to present experiments.

As mentioned, Wigger *et al.* [36] show that a $\omega_b = 2.9$ μeV surface acoustic wave (SAW) was coupled to 1.36-eV In(Ga)As QDs (this is the bare bright exciton energy ω_X) embedded in Bragg mirrors and illuminated by an external laser whose energy can be finely tuned piezoelectrically. This is exactly the experimental setup needed for the proposal we make in this work, which is why we assume this value for the frequency of the acoustic cavity.

The internal structure of the QD remains unchanged, meaning that the δ parameters of the QD [cf. Eq. (2)] are $\delta_0 = 69.0\omega_b$, $\delta_1 = 62.1\omega_b$, and $\delta_2 = 17.2\omega_b$, which, again, match the values reported by Bayer *et al.* [46]. Note that the ratios have changed with respect to those reported in the main text because we assumed a new value of ω_b, but energetically the values remain the same.

The quality factor of the SAW determines the phonon escape rate from the phonon cavity defined by the SAW. This rate is associated with an energy $\kappa = 10.9$ neV [39], which can be achieved by further confining the phonon mode using lateral phononic crystals.

Regarding the external laser, its power can be used to tune the effective laser amplitude Ω_1. It is well known that such an amplitude is related to the square of the laser power [81,82]. Thus, we set $\Omega_1 \approx 4.69\omega_b \in [0.1\ \mu\text{eV}, 200\ \mu\text{eV}]$, where the energy range is a reasonable experimental range according to Kamada *et al.* [81]. All parameters given in an interval are tuned to minimize the generalized second-order two-phonon bundle correlation function, as explained in Ref. [62].

The dissipative processes involving the QD are exciton decay and dephasing. As mentioned in Sec. III, the decay rate of dark excitons is lower than that of bright excitons because it involves a random spin flip before spontaneous emission can occur. Moreover, it has been demonstrated that the exciton decay rates (both bright and dark) can be inhibited or enhanced through optical and electrical control: i.e., embedding the QDs in different optical cavities, and by controlling electric fields with external gates [83–86]. Thus, for the bright-exciton decay rate, we consider it to be $\gamma_b \approx 0.01\omega_b \in [0.01\omega_b, 1.5\omega_b]$. This is 2 orders of magnitude below the assumed value in the experiment by Wigger *et al.* [36]. Nonetheless, we argue that a better optical cavity that minimizes the coupling of the QD bright excitons to optical leaky modes [55] (thus, generating an optical band gap) can allow experimental physicists to achieve significantly lower exciton decay rates, such as in the work by Lodahl *et al.* [86]. As shown in the experiment by Dalgarno *et al.* [83], the dark-exciton decay can be tuned

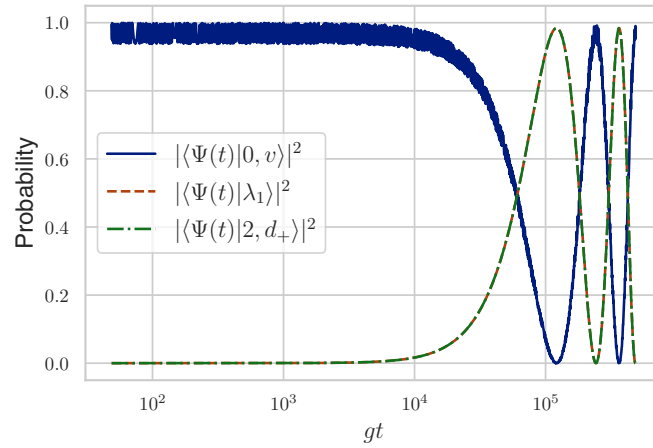

FIG. 7. Giant Rabi oscillations between the state $|0, v\rangle$ and $|\lambda_1\rangle \approx |2, d_+\rangle$. As in Fig. 3, we plot the occupation of the states $|0, v\rangle$ (solid line), $|\lambda_1\rangle$ (dashed line), and $|2, d_+\rangle$ (dot-dashed line). In this regime of strong driving and weak coupling, the laser detuning is $\Delta/\omega_b = (\omega_X - \omega_L)/\omega_b \approx 57.82$.

to be 1 or 2 orders of magnitude lower than that of the bright exciton, which is why we stick to the assumed value in Sec. III, i.e., $\gamma_d = 0.1\gamma_b$. Finally, the pure dephasing rate is assumed to be $\gamma_\phi \approx 0.123\omega_b \in [0.1\omega_b, 2\omega_b]$. Pure dephasing is associated with the coupling of the QDs' exciton to the QDs' own lattice phonons [87–89]. The low-temperature broadening has been measured to be on the order of 0.1–1 μeV [90,91]. Perhaps, pure dephasing is the parameter that is most difficult to control; however, we point out that recent experiments have shown interesting control mechanisms for pure dephasing in QDs [92].

Lastly, the coupling between the confined phonon mode and the QD excitons was assumed to be $g = g_{\text{bb}} = g_{\text{bd}} \approx 0.02\omega_b \in [0.01\omega_b, \omega_b]$, which is in the order of tens of nanoelectronvolts. A similar, but smaller, magnitude has been determined in experiments where phonon modes are coherently coupled to QDs [38]. This experiment also displays a similar frequency-to-coupling constant ratio (only 1 order of magnitude higher than ours). However, we stress that QD coupling to SAW modes can reach larger values, depending on where the QDs are placed: placing them at the nodes of the phonon cavity will yield no coupling, whereas placing them at the antinodes will yield the maximum coupling [80,93].

Given the values of the parameters that specify the physical system, we show in Fig. 7 that it is also possible to produce giant Rabi oscillations between a state mostly composed of the vacuum state $|0, v\rangle$ and the two-phonon dark symmetric state $|\lambda_1\rangle \approx |2, d_+\rangle$. The reason why the $|0, v\rangle$ population shows an additional oscillation is because, for the specified set of parameters, $|0, v\rangle$ is not an eigenstate of the Hamiltonian. Instead, the giant Rabi oscillations occur, at a specified laser detuning, between the degenerate eigenstates $|\lambda_0\rangle$—which has a dominant component $|0, v\rangle$—and $|\lambda_1\rangle$. Furthermore, the generalized second-order two-phonon bundle correlation function has a value of 0.39, which is well within the anti-bunching quantum regime.

[1] A. A. Balandin, Nanophononics: Phonon engineering in nanostructures and nanodevices, J. Nanosci. Nanotechnol. **5**, 1015 (2005).

[2] R. Manenti, A. F. Kockum, A. Patterson, T. Behrle, J. Rahamim, G. Tancredi, F. Nori, and P. J. Leek, Circuit quantum acoustodynamics with surface acoustic waves, Nat. Commun. **8**, 975 (2017).

[3] J. Zhang, M. Um, D. Lv, J.-N. Zhang, L.-M. Duan, and K. Kim, NOON States of Nine Quantized Vibrations in Two Radial Modes of a Trapped Ion, Phys. Rev. Lett. **121**, 160502 (2018).

[4] M. J. A. Schuetz, E. M. Kessler, G. Giedke, L. M. K. Vandersypen, M. D. Lukin, and J. I. Cirac, Universal Quantum Transducers Based on Surface Acoustic Waves, Phys. Rev. X **5**, 031031 (2015).

[5] A. Noguchi, R. Yamazaki, Y. Tabuchi, and Y. Nakamura, Qubit-Assisted Transduction for a Detection of Surface Acoustic Waves near the Quantum Limit, Phys. Rev. Lett. **119**, 180505 (2017).

[6] P. Arrangoiz-Arriola, E. A. Wollack, M. Pechal, J. D. Witmer, J. T. Hill, and A. H. Safavi-Naeini, Coupling a Superconducting Quantum Circuit to a Phononic Crystal Defect Cavity, Phys. Rev. X **8**, 031007 (2018).

[7] A. Ask, M. Ekström, P. Delsing, and G. Johansson, Cavity-free vacuum-Rabi splitting in circuit quantum acoustodynamics, Phys. Rev. A **99**, 013840 (2019).

[8] U. von Lüpke, Y. Yang, M. Bild, L. Michaud, M. Fadel, and Y. Chu, Parity measurement in the strong dispersive regime of circuit quantum acoustodynamics, Nat. Phys. (2022), doi: 10.1038/s41567-022-01591-2.

[9] D. E. Reiter, T. Kuhn, and V. M. Axt, Distinctive characteristics of carrier-phonon interactions in optically driven semiconductor quantum dots, Adv. Phys.: X **4**, 1655478 (2019).

[10] M. Weiß and H. J. Krenner, Interfacing quantum emitters with propagating surface acoustic waves, J. Phys. D **51**, 373001 (2018).

[11] Q. Bin, X.-Y. Lü, F. P. Laussy, F. Nori, and Y. Wu, *N*-Phonon Bundle Emission via the Stokes Process, Phys. Rev. Lett. **124**, 053601 (2020).

[12] K. Wan, S. Choi, I. H. Kim, N. Shutty, and P. Hayden, Fault-tolerant qubit from a constant number of components, PRX Quantum **2**, 040345 (2021).

[13] D. T. Bell and R. C. Li, Surface-acoustic-wave resonators, Proc. IEEE **64**, 711 (1976).

[14] E. M. Weig, R. H. Blick, T. Brandes, J. Kirschbaum, W. Wegscheider, M. Bichler, and J. P. Kotthaus, Single-Electron-Phonon Interaction in a Suspended Quantum Dot Phonon Cavity, Phys. Rev. Lett. **92**, 046804 (2004).

[15] G. Rozas, M. F. P. Winter, B. Jusserand, A. Fainstein, B. Perrin, E. Semenova, and A. Lemaître, Lifetime of THz Acoustic Nanocavity Modes, Phys. Rev. Lett. **102**, 015502 (2009).

[16] O. O. Soykal, R. Ruskov, and C. Tahan, Sound-Based Analogue of Cavity Quantum Electrodynamics in Silicon, Phys. Rev. Lett. **107**, 235502 (2011).

[17] A. Fainstein, N. D. Lanzillotti-Kimura, B. Jusserand, and B. Perrin, Strong Optical-Mechanical Coupling in a Vertical GaAs/AlAs Microcavity for Subterahertz Phonons and Near-Infrared Light, Phys. Rev. Lett. **110**, 037403 (2013).

[18] P. Kharel, Y. Chu, M. Power, W. H. Renninger, R. J. Schoelkopf, and P. T. Rakich, Ultra-high-*Q* phononic resonators on-chip at cryogenic temperatures, APL Photonics **3**, 066101 (2018).

[19] A. N. Bolgar, J. I. Zotova, D. D. Kirichenko, I. S. Besedin, A. V. Semenov, R. S. Shaikhaidarov, and O. V. Astafiev, Quantum Regime of a Two-Dimensional Phonon Cavity, Phys. Rev. Lett. **120**, 223603 (2018).

[20] H. Chen, N. F. Opondo, B. Jiang, E. R. MacQuarrie, R. S. Daveau, S. A. Bhave, and G. D. Fuchs, Engineering electron–phonon coupling of quantum defects to a semiconfocal acoustic resonator, Nano Letters, Nano Lett. **19**, 7021 (2019).

[21] V. J. Gokhale, B. P. Downey, D. S. Katzer, N. Nepal, A. C. Lang, R. M. Stroud, and D. J. Meyer, Epitaxial bulk acoustic wave resonators as highly coherent multi-phonon sources for quantum acoustodynamics, Nat. Commun. **11**, 2314 (2020).

[22] S. Sandeep, S. L. Heywood, R. P. Campion, A. J. Kent, and R. N. Kini, Resonance of terahertz phonons in an acoustic nanocavity, Phys. Rev. B **98**, 235303 (2018).

[23] M. K. Zalalutdinov, J. T. Robinson, J. J. Fonseca, S. W. LaGasse, T. Pandey, L. R. Lindsay, T. L. Reinecke, D. M. Photiadis, J. C. Culbertson, C. D. Cress, and B. H. Houston, Acoustic cavities in 2D heterostructures, Nat. Commun. **12**, 3267 (2021).

[24] G. S. MacCabe, H. Ren, J. Luo, J. D. Cohen, H. Zhou, A. Sipahigil, M. Mirhosseini, and O. Painter, Nano-acoustic resonator with ultralong phonon lifetime, Science **370**, 840 (2020).

[25] Y. Chu, P. Kharel, W. H. Renninger, L. D. Burkhart, L. Frunzio, P. T. Rakich, and R. J. Schoelkopf, Quantum acoustics with superconducting qubits, Science **358**, 199 (2017).

[26] A. D. O'Connell, M. Hofheinz, M. Ansmann, R. C. Bialczak, M. Lenander, E. Lucero, M. Neeley, D. Sank, H. Wang, M. Weides, J. Wenner, J. M. Martinis, and A. N. Cleland, Quantum ground state and single-phonon control of a mechanical resonator, Nature (London) **464**, 697 (2010).

[27] P. V. Santos, M. Msall, and S. Ludwig, Acoustic field for the control of electronic excitations in semiconductor nanostructures, in *Proceedings of the 2018 IEEE International Ultrasonics Symposium (IUS)* (IEEE, New York, 2018), pp. 1–4.

[28] J. M. Pirkkalainen, S. U. Cho, J. Li, G. S. Paraoanu, P. J. Hakonen, and M. A. Sillanpää, Hybrid circuit cavity quantum electrodynamics with a micromechanical resonator, Nature (London) **494**, 211 (2013).

[29] M. D. LaHaye, J. Suh, P. M. Echternach, K. C. Schwab, and M. L. Roukes, Nanomechanical measurements of a superconducting qubit, Nature (London) **459**, 960 (2009).

[30] M. V. Gustafsson, T. Aref, A. F. Kockum, M. K. Ekström, G. Johansson, and P. Delsing, Propagating phonons coupled to an artificial atom, Science **346**, 207 (2014).

[31] C. F. Ockeloen-Korppi, E. Damskägg, J.-M. Pirkkalainen, T. T. Heikkilä, F. Massel, and M. A. Sillanpää, Noiseless Quantum Measurement and Squeezing of Microwave Fields Utilizing Mechanical Vibrations, Phys. Rev. Lett. **118**, 103601 (2017).

[32] F. Massel, T. T. Heikkilä, J. M. Pirkkalainen, S. U. Cho, H. Saloniemi, P. J. Hakonen, and M. A. Sillanpää, Microwave amplification with nanomechanical resonators, Nature (London) **480**, 351 (2011).

[33] F. Rouxinol, Y. Hao, F. Brito, A. O. Caldeira, E. K. Irish, and M. D. LaHaye, Measurements of nanoresonator-qubit interactions in a hybrid quantum electromechanical system, Nanotechnology **27**, 364003 (2016).

[34] T. F. Li, Y. A. Pashkin, O. Astafiev, Y. Nakamura, J. S. Tsai, and H. Im, High-frequency metallic nanomechanical resonators, Appl. Phys. Lett. **92**, 043112 (2008).

[35] E. Stock, M.-R. Dachner, T. Warming, A. Schliwa, A. Lochmann, A. Hoffmann, A. I. Toropov, A. K. Bakarov, I. A. Derebezov, M. Richter, V. A. Haisler, A. Knorr, and D. Bimberg, Acoustic and optical phonon scattering in a single In(Ga)As quantum dot, Phys. Rev. B **83**, 041304(R) (2011).

[36] D. Wigger, M. Weiß, M. Lienhart, K. Müller, J. J. Finley, T. Kuhn, H. J. Krenner, and P. Machnikowski, Resonance-fluorescence spectral dynamics of an acoustically modulated quantum dot, Phys. Rev. Research **3**, 033197 (2021).

[37] A. Vartanian, A. Kirakosyan, and K. Vardanyan, Spin relaxation mediated by spin-orbit and acoustic phonon interactions in a single-electron two-dimensional quantum dot, Superlattices Microstruct. **122**, 548 (2018).

[38] J. Kettler, N. Vaish, L. M. de Lépinay, B. Besga, P.-L. de Assis, O. Bourgeois, A. Auffèves, M. Richard, J. Claudon, J.-M. Gérard, B. Pigeau, O. Arcizet, P. Verlot, and J.-P. Poizat, Inducing micromechanical motion by optical excitation of a single quantum dot, Nat. Nanotechnol. **16**, 283 (2021).

[39] Y. Xu, W. Fu, C.-l. Zou, Z. Shen, and H. X. Tang, High quality factor surface Fabry-Perot cavity of acoustic waves, Appl. Phys. Lett. **112**, 073505 (2018).

[40] A. V. Akimov, C. L. Poyser, and A. J. Kent, Review of microwave electro-phononics in semiconductor nanostructures, Semicond. Sci. Technol. **32**, 053003 (2017).

[41] G. L. Bir and G. E. Pikus, *Symmetry and Strain-Induced Effects in Semiconductors* (Wiley, New York, 1974).

[42] C. A. Jiménez-Orjuela, H. Vinck-Posada, and J. M. Villas-Bôas, Dark excitons in a quantum-dot–cavity system under a tilted magnetic field, Phys. Rev. B **96**, 125303 (2017).

[43] M. Neumann, F. Kappe, T. K. Bracht, M. Cosacchi, T. Seidelmann, V. M. Axt, G. Weihs, and D. E. Reiter, Optical stark shift to control the dark exciton occupation of a quantum dot in a tilted magnetic field, Phys. Rev. B **104**, 075428 (2021).

[44] C. Adambukulam, V. Sewani, H. Stemp, S. Asaad, M. Madzik, A. Morello, and A. Laucht, An ultra-stable 1.5 T permanent magnet assembly for qubit experiments at cryogenic temperatures, Rev. Sci. Instrum. **92**, 085106 (2021).

[45] S. Nomura, Y. Segawa, and T. Kobayashi, Confined excitons in a semiconductor quantum dot in a magnetic field, Phys. Rev. B **49**, 13571 (1994).

[46] M. Bayer, G. Ortner, O. Stern, A. Kuther, A. A. Gorbunov, A. Forchel, P. Hawrylak, S. Fafard, K. Hinzer, T. L. Reinecke, S. N. Walck, J. P. Reithmaier, F. Klopf, and F. Schäfer, Fine structure of neutral and charged excitons in self-assembled In(Ga)As/(Al)GaAs quantum dots, Phys. Rev. B **65**, 195315 (2002).

[47] T. Belhadj, C.-M. Simon, T. Amand, P. Renucci, B. Chatel, O. Krebs, A. Lemaître, P. Voisin, X. Marie, and B. Urbaszek, Controlling the Polarization Eigenstate of a Quantum Dot Exciton with Light, Phys. Rev. Lett. **103**, 086601 (2009).

[48] L. M. Woods, T. L. Reinecke, and R. Kotlyar, Hole spin relaxation in quantum dots, Phys. Rev. B **69**, 125330 (2004).

[49] T. Takagahara, Effects of dielectric confinement and electron-hole exchange interaction on excitonic states in semiconductor quantum dots, Phys. Rev. B **47**, 4569 (1993).

[50] K. Roszak, V. M. Axt, T. Kuhn, and P. Machnikowski, Exciton spin decay in quantum dots to bright and dark states, Phys. Rev. B **76**, 195324 (2007).

[51] Note that the ground state is not exactly $|0, v\rangle$, because the states are dressed by the external laser.

[52] H.-P. Breuer and F. Petruccione, *The Theory of Open Quantum Systems* (Oxford University Press on Demand, 2002).

[53] G. Lindblad, On the generators of quantum dynamical semigroups, Commun. Math. Phys. **48**, 119 (1976).

[54] V. Gorini, A. Kossakowski, and E. C. G. Sudarshan, Completely positive dynamical semigroups of *N*-level systems, J. Math. Phys. **17**, 821 (1976).

[55] J. I. Perea, D. Porras, and C. Tejedor, Dynamics of the excitations of a quantum dot in a microcavity, Phys. Rev. B **70**, 115304 (2004).

[56] M. F. Pascual Winter, G. Rozas, A. Fainstein, B. Jusserand, B. Perrin, A. Huynh, P. O. Vaccaro, and S. Saravanan, Selective Optical Generation of Coherent Acoustic Nanocavity Modes, Phys. Rev. Lett. **98**, 265501 (2007).

[57] S. Crooker, T. Barrick, J. Hollingsworth, and V. Klimov, Multiple temperature regimes of radiative decay in CdSe nanocrystal quantum dots: Intrinsic limits to the dark-exciton lifetime, Appl. Phys. Lett. **82**, 2793 (2003).

[58] T. Takagahara, Theory of exciton dephasing in semiconductor quantum dots, in *Semiconductor Quantum Dots*, edited by Y. Masumoto and T. Takagahara (Springer, Berlin, 2002), pp. 353–388.

[59] J. Dalibard, Y. Castin, and K. Mølmer, Wave-Function Approach to Dissipative Processes in Quantum Optics, Phys. Rev. Lett. **68**, 580 (1992).

[60] K. Mølmer, Y. Castin, and J. Dalibard, Monte Carlo wave-function method in quantum optics, J. Opt. Soc. Am. B **10**, 524 (1993).

[61] C. S. Muñoz, E. Del Valle, A. G. Tudela, K. Müller, S. Lichtmannecker, M. Kaniber, C. Tejedor, J. Finley, and F. Laussy, Emitters of N*N*, Nat. Photonics **8**, 550 (2014).

[62] Parameters can be tuned to get a larger amount of two-phonon emission processes. In this work, we tuned parameters with the tree-structured Parzen estimator implemented in OPTUNA [94] to minimize the generalized second-order two-phonon bundle correlation function at a value for the laser detuning that coupled the vacuum and the $|2, d_+\rangle$ state through giant Rabi oscillations.

[63] F. Dell'Anno, S. De Siena, and F. Illuminati, Multiphoton quantum optics and quantum state engineering, Phys. Rep. **428**, 53 (2006).

[64] R. H. Brown and R. Q. Twiss, Correlation between photons in two coherent beams of light, Nature (London) **177**, 27 (1956).

[65] R. J. Glauber, The quantum theory of optical coherence, Phys. Rev. **130**, 2529 (1963).

[66] X. T. Zou and L. Mandel, Photon-antibunching and sub-Poissonian photon statistics, Phys. Rev. A **41**, 475 (1990).

[67] B. R. Mollow, Power spectrum of light scattered by two-level systems, Phys. Rev. **188**, 1969 (1969).

[68] V. Vargas-Calderón and H. Vinck-Posada, Phonon-assisted tunnelling in a double quantum dot molecule immersed in a cavity, Optik **183**, 168 (2019).

[69] T. Petrosky and I. Prigogine, The Liouville space extension of quantum mechanics, in *Advances in Chemical Physics* (Wiley & Sons, New York, 1996), pp. 1–120.

[70] T. Petrosky, Complex spectral representation of the Liouvillian and kinetic Theory in nonequilibrium physics, Prog. Theor. Phys. **123**, 395 (2010).

[71] D. Manzano and P. Hurtado, Harnessing symmetry to control quantum transport, Adv. Phys. **67**, 1 (2018).

[72] V. V. Albert and L. Jiang, Symmetries and conserved quantities in Lindblad master equations, Phys. Rev. A **89**, 022118 (2014).

[73] N. Hatano and T. Petrosky, Eigenvalue problem of the Liouvillian of open quantum systems, AIP Conf. Proc. **1648**, 200005 (2015).

[74] V. Vargas-Calderón, Phonon-assisted tunnelling in double quantum dot molecules immersed in a microcavity, Thesis, Research Gate 10.13140/RG.2.2.31486.23360/1 (2018).

[75] B. A. Tay and T. Petrosky, Biorthonormal eigenbasis of a Markovian master equation for the quantum Brownian motion, J. Math. Phys. **49**, 113301 (2008).

[76] J. M. Torres, Closed-form solution of lindblad master equations without gain, Phys. Rev. A **89**, 052133 (2014).

[77] S. Echeverri-Arteaga, H. Vinck-Posada, and E. A. Gómez, Explanation of the quantum phenomenon of off-resonant cavity-mode emission, Phys. Rev. A **97**, 043815 (2018).

[78] V. Vargas-Calderón and H. Vinck-Posada, Light emission properties in a double quantum dot molecule immersed in a cavity: Phonon-assisted tunneling, Phys. Lett. A **384**, 126076 (2020).

[79] C. Sánchez Muñoz, F. P. Laussy, E. del Valle, C. Tejedor, and A. González-Tudela, Filtering multiphoton emission from state-of-the-art cavity quantum electrodynamics, Optica **5**, 14 (2018).

[80] E. D. S. Nysten, A. Rastelli, and H. J. Krenner, A hybrid (Al)GaAs-$LiNbO_3$ surface acoustic wave resonator for cavity quantum dot optomechanics, Appl. Phys. Lett. **117**, 121106 (2020).

[81] H. Kamada, H. Gotoh, J. Temmyo, T. Takagahara, and H. Ando, Exciton Rabi Oscillation in a Single Quantum Dot, Phys. Rev. Lett. **87**, 246401 (2001).

[82] G. Khitrova, H. M. Gibbs, M. Kira, S. W. Koch, and A. Scherer, Vacuum Rabi splitting in semiconductors, Nat. Phys. **2**, 81 (2006).

[83] P. A. Dalgarno, J. M. Smith, B. D. Gerardot, A. O. Govorov, K. Karrai, P. M. Petroff, and R. J. Warburton, Dark exciton decay dynamics of a semiconductor quantum dot, Phys. Status Solidi A **202**, 2591 (2005).

[84] A. Laucht, F. Hofbauer, N. Hauke, J. Angele, S. Stobbe, M. Kaniber, G. Böhm, P. Lodahl, M.-C. Amann, and J. J. Finley, Electrical control of spontaneous emission and strong coupling for a single quantum dot, New J. Phys. **11**, 023034 (2009).

[85] L. Li, W. Wang, T. S. Luk, X. Yang, and J. Gao, Enhanced quantum dot spontaneous emission with multilayer metamaterial nanostructures, ACS Photonics **4**, 501 (2017).

[86] P. Lodahl, A. Floris van Driel, I. S. Nikolaev, A. Irman, K. Overgaag, D. Vanmaekelbergh, and W. L. Vos, Controlling the dynamics of spontaneous emission from quantum dots by photonic crystals, Nature (London) **430**, 654 (2004).

[87] T. Takagahara, Theory of exciton dephasing in semiconductor quantum dots, Phys. Rev. B **60**, 2638 (1999).

[88] L. Besombes, K. Kheng, L. Marsal, and H. Mariette, Acoustic phonon broadening mechanism in single quantum dot emission, Phys. Rev. B **63**, 155307 (2001).

[89] E. A. Muljarov and R. Zimmermann, Dephasing in Quantum Dots: Quadratic Coupling to Acoustic Phonons, Phys. Rev. Lett. **93**, 237401 (2004).

[90] P. Borri, W. Langbein, S. Schneider, U. Woggon, R. L. Sellin, D. Ouyang, and D. Bimberg, Ultralong Dephasing Time in InGaAs Quantum Dots, Phys. Rev. Lett. **87**, 157401 (2001).

[91] C. Kammerer, C. Voisin, G. Cassabois, C. Delalande, P. Roussignol, F. Klopf, J. P. Reithmaier, A. Forchel, and J. M. Gérard, Line narrowing in single semiconductor quantum dots: Toward the control of environment effects, Phys. Rev. B **66**, 041306(R) (2002).

[92] J. Liu, S. V. Kilina, S. Tretiak, and O. V. Prezhdo, Ligands slow down pure-dephasing in semiconductor quantum dots, ACS Nano **9**, 9106 (2015).

[93] E. D. S. Nysten, Y. H. Huo, H. Yu, G. F. Song, A. Rastelli, and H. J. Krenner, Multi-harmonic quantum dot optomechanics in fused $LiNbO_3$-(Al)GaAs hybrids, J. Phys. D **50**, 43LT01 (2017).

[94] T. Akiba, S. Sano, T. Yanase, T. Ohta, and M. Koyama, Optuna: A next-generation hyperparameter optimization framework, in *Proceedings of the 25rd ACM SIGKDD International Conference on Knowledge Discovery and Data Mining* (ACM, New York, 2019).